

LASER-DRIVEN ELECTRON BEAMS IN MATTER

L. Volpe,¹ G. Birindelli,¹ D. Batani,¹ A. Morace,¹ P. Carpegiani,¹ M. H. Xu,² F. Liu,² Y. Zhang,²
Z. Zhang,² X. X. Lin,² F. Liu,² S. J. Wang,² P. F. Zhu,² L. M. Meng,² Z. H. Wang,² Y. T. Li,²
Z. M. Sheng,² Z. Y. Wei,² J. Zhang,² L. Gremillet³

¹ Universitá degli Studi di Milano-Bicocca, Piazza della scienza 3, Milano 20126 Italy;

² Institute of Physics, Chinese Academy of Sciences, P.O. Box 603, Beijing 100080, China;

³ CEA, Bruyeres le Chatel, France

Introduction

The knowledge of the physics of fast electrons transport in matter is crucial in order to assess the feasibility of the fast ignition (FI) approach to Inertial Confinement Fusion [1]. Indeed, FI depends on the generation of hot electrons, their collimation, transport, and energy deposition in the over-dense region of the plasma. The estimation of hot electron stopping length and factors affecting it, are therefore, extremely important. In the last 10 years many papers have been devoted to the study of fast electron transport in metals [2, 3], insulators [4], shocked material [5], foams [6], gas [7]. In this paper we report about an experiment performed at the the 50 fs laser facility "Xtreme Light XL-III" of the Institute of Physics of the Chinese Academy of Sciences in Beijing. The aim of the experiment was to investigated the production and propagation of fast electrons accelerated by laser pulse focused on solid targets, with a typical intensity ranging between of 10^{17-19} W/cm². Aluminium targets with different thicknesses (from 1 to 10 μ m) have been used in order to investigate the penetration ranges and the role of density and electric conductivity on fast electron transport. All targets had a tracer layer of 3 μ m Cu inside. The propagation of fast electrons through this layer induces the emission of X-ray photons at the characteristic Cu- K_{α} line. We then used a spherically bent Bragg crystal to obtain a spatially resolved image of the Cu K_{α} spot on the target, which reflects the distribution of fast electrons at the rear side. The front side emission of the target was collected by a pinhole camera and an HOPG spectrometer has been used to collect the K_{α} signal on the back side of the target. The penetration ranges found for aluminium is compatible with the fast electron temperature of 400 keV, corresponding to what can be obtained from published scaling laws based on resonant absorption [3]. Finally, we measured the spot size and the integrated signal as a function of the thickness and the efficiency of conversion from laser energy to fast electron energy.

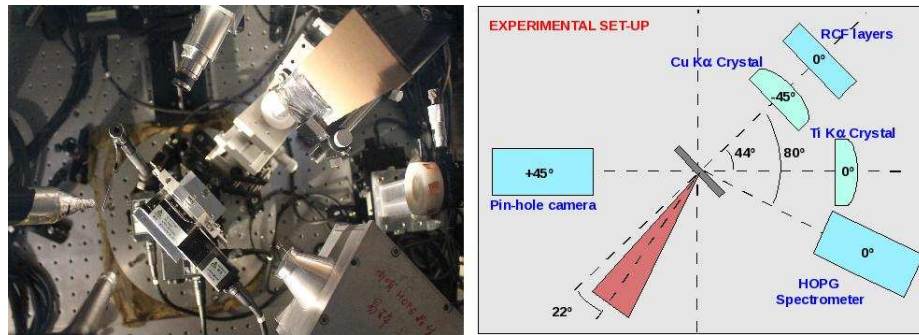


Figure 1: (left) top view picture of the interaction chamber. (right) top view schematic of the interaction chamber

Laser system and experimental set-up

Targets were irradiated at the 50 fs laser facility "Xtreme Light XL-III" of the Institute of Physics of the Chinese Academy of Sciences in Beijing, a Ti:Sa laser source emitting at 800 nm. During the experimental campaign some technical problems to the laser system have strongly reduced the operating laser energy ($E_L \sim 2J$) and the number of irradiated targets. The laser beam was impinging on target at an angle of 22.5° from the normal and was focused with an F/3 off-axis parabola to a spot with an effective radius $R \leq 10 \mu\text{m}$. Hence the targets were typically irradiated at an intensity of $\sim 10^{19} \text{ W/cm}^2$. The pre-pulse effects are avoided using the Optical Parameter Amplification (OPA) technique. In the experiment we used two types of targets: the first one made of a single-layer of copper (test targets), the latter made by three layers: aluminium (1,6,10 μm propagation layer), copper (3 μm tracer layer) and aluminium (1 μm). The experimental set-up is shown in Fig.1.

Diagnostics

Several diagnostics were used in the experiment:

X-ray pin hole camera: A X-ray pin hole camera coupled to a CCD detector was pointed at the front face of the target, where the laser-matter interaction takes place, with an angle of 45° both in the vertical and horizontal plane. The magnification of the x-ray spot was 13X.

Spherical crystal for X-ray imaging: Cu K α photons are emitted as fast electrons cross the Cu tracer layer on the target rear side. Such photons were detected using a spherically bent Bragg crystal [8] coupled to a X-ray CCD. The spherical crystal combines the reflecting properties, typical of a Bragg crystal, to the focusing properties of a spherical mirror. In this experiment we have used two different crystals: Quartz 211 and 203 with spacing $2d=3.082 \text{ \AA}$ and $2d=2.749 \text{ \AA}$ as needed to detect Cu and Ti K α photons ($E=8048 \text{ eV}$ $E=4.512 \text{ eV}$) at the Bragg angles

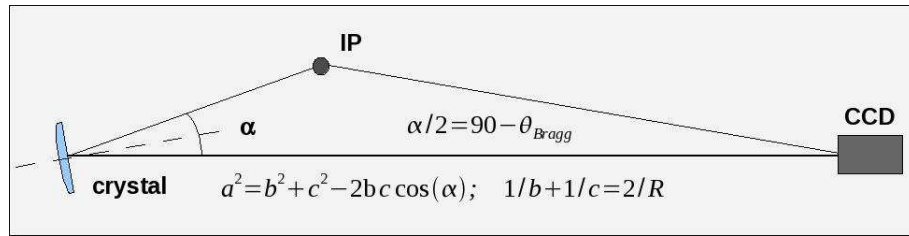


Figure 2: scheme of typical planar alignment and constraint between crystal, ccd, interaction point

$\theta_{Bragg} = (88.6)^\circ$ and $\theta_{Bragg} = (88.9)^\circ$ in the second and in the first order. The condition of using a nearly 90° Bragg angle comes from the need of reducing astigmatism in the produced image [8]. The radius of curvature of the crystals is 380 mm. Fig. 2 shows the alignment constraint between crystal, ccd camera and interaction point. Following the rules in fig. 2 we choose the crystal-interaction point distance 231 mm obtaining an image with a magnification of 4.6 X onto the CCD placed at 1070 mm. This diagnostics allows obtaining a spectrally and spatially resolved X-ray image of the K_α spot on target rear side, reproducing the spatial shape of the fast electron beam. From the ccd signal we can obtain two types of quantitative information: the spot size diameter and the total K_α signal (by integrating the signal counts on the whole image). The spot size, measured as a function of target thickness, can be used to evaluate the angle of divergence of fast electron beam. Instead from the integrated signal as a function of target areal density, it is possible to calculate the penetration depth of fast electrons. Also, it is possible, with some reasonable assumptions, to estimate the total energy in the fast electron beam thereby allowing evaluating the efficiency of conversion from laser energy to fast electrons.

HOPG spectrometer An Highly Ordered Pyrolytic Graphite (HOPG)x-ray spectrometer, operating in a energy range between 6.9 keV to 9.1 keV, has been used to collect the X-ray Cu K_α lines.

Experimental results and conclusions

Fig. 3 shows a set of typical results (a) K_α spot, (b) pin hole camera images and (c) HOPG spectrometer K_α line . We have performed a preliminary analysis of the experimental results.

- we estimate the divergence of the electron beam plotting the FWHM of the K_α spot (es. fig 3(a)) as a function of the propagation layer thickness obtaining a value about 80 degree according to that was obtained in other experiment involving small thickness targets.

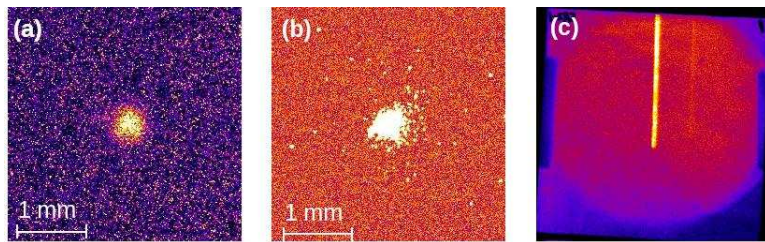


Figure 3: Typical result obtained with Al(1 μ m)-Cu(3 μ m)-Al(1 μ m) target, laser energy $E_L = 2.9$ J and Intensity $I = 1.8 \times 10^{19}$ W/cm². (a) K_α spot, (b) pin hole camera images and (c) HOPG spectrometer K_α line (integrated signal from 4 repeated shot).

- we estimate the penetration depth from the K_α integrated signal obtaining a value about 90 μ m, then using the Beg Scaling law $T = 100KeV(I\lambda^2)^{1/3}$ [3] we obtain a mean electron temperature about $T \simeq 400$ KeV. This value is compatible with the collisional stopping power of electrons in aluminium obtained in [9]. The inhibition effects of the electrons self-generated electric field [?] can be neglected in this particular case since the penetration range due to that field is about 200 μ m i.e. greater than the collisional one.
- starting from the K_α integrated signal and using Beg scaling law it is possible to estimate the fraction of laser energy which is transferred to electrons [11]. It seems that the conversion efficiency is under 10 %.

References

- [1] M Tabak et al Phys. Of Plasmas, 1, 1626-1634 (1994)
- [2] M Key et al Phys. of Plasma, 5 1966 (1998); Wharton Phys. Rev. Lett. 81, 822-825 (1998)
- [3] F N Beg Phys. Plasmas 4, 447 (1997);
- [4] F. Pisani et al Phys. Rev. E 62, R5927 (2000).
- [5] Hall, Batani, Santos
- [6] D. Batani et al Phys. Rev. E 62, 8573 (2000)
- [7] D. Batani et al Phys. Rev. Lett. 94, 055004 (2005)
- [8] J A Koch et al Review of Scientific Instrument 74 3 (2003)
- [9] NIST: Stopping power and Range tables for electrons table: www.physics.nist.gov
- [10] A R Bell et al 1997 Plasma Phys. Control. Fusion 39 653
- [11] A. Morace, D. Batani NIMA Volume 623, Issue 2, 11 2010, Pages 797-800